

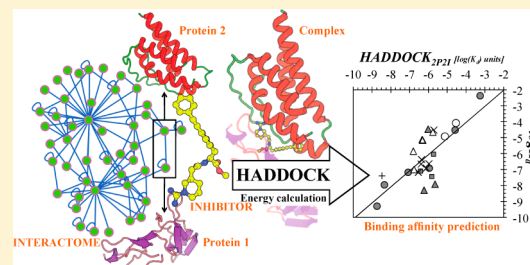
# HADDOCK<sub>2P2I</sub>: A Biophysical Model for Predicting the Binding Affinity of Protein–Protein Interaction Inhibitors

Panagiotis L. Kastritis,<sup>†</sup> João P. G. L. M. Rodrigues, and Alexandre M. J. J. Bonvin\*

Bijvoet Center for Biomolecular Research, Faculty of Science/Chemistry, Utrecht University, Utrecht, 3584CH, the Netherlands

## Supporting Information

**ABSTRACT:** The HADDOCK score, a scoring function for both protein–protein and protein–nucleic acid modeling, has been successful in selecting near-native docking poses in a variety of cases, including those of the CAPRI blind prediction experiment. However, it has yet to be optimized for small molecules, and in particular inhibitors of protein–protein interactions, that constitute an “unmined gold reserve” for drug design ventures. We describe here HADDOCK<sub>2P2I</sub>, a biophysical model capable of predicting the binding affinity of protein–protein complex inhibitors close to experimental error (~2-fold larger). The algorithm was trained and 4-fold cross-validated against experimental data for 27 inhibitors targeting 7 protein–protein complexes of various functions and tested on an independent set of 24 different inhibitors for which  $K_d$ /IC<sub>50</sub> data are available. In addition, two popular ligand topology generation and parametrization methods (ACPYPE and PRODRG) were assessed. The resulting HADDOCK<sub>2P2I</sub> model, derived from the original HADDOCK score, provides insights into inhibition determinants: while the role of electrostatics and desolvation energies is case-dependent, the interface area plays a more critical role compared to protein–protein interactions.



## INTRODUCTION

Protein–protein interactions (PPIs) define most of the cellular processes in the cell,<sup>1</sup> such as differentiation, proliferation, signal transduction, and apoptosis. Being able to design PPI inhibitors will drastically catalyze the development of novel therapeutics for diseases, such as cancer.<sup>2</sup> Such inhibitors are currently considered “an unmined gold reserve”<sup>3</sup> for drug design in general. Consequently, novel software tools are being developed and made publicly available that target the design of inhibitor of PPIs, such as PocketQuery.<sup>4–6</sup> The chemical space of PPI inhibitors is, however, rather unique.<sup>7–9</sup> Protein–protein interfaces have been manually curated and collected in several dedicated databases, such as iPPi-DB,<sup>10</sup> a database that includes associated pharmacological data, and the 2P2I database.<sup>11,12</sup> Recent studies on a structure-based benchmark<sup>11</sup> of PPI inhibitors (collected from the 2P2I database<sup>12</sup>) showed that the size of the ligands targeting the interface of protein–protein complexes is substantially larger than that of normal inhibitors that target the active site of single molecules like enzymes<sup>9</sup> and suggest that PPI inhibitors are mainly large, lipophilic, and aromatic compounds. Because of the different nature of the target interface and ligands, dedicated biophysical models are needed to predict the binding affinity of PPI inhibitors. Although current biophysical models have proven to reasonably approximate the affinity of protein–ligand complexes,<sup>9,13</sup> these have yet to be optimized to predict the affinity of PPI inhibitors. A drop by more than 10% in docking success rates is reported when inhibitors of protein–protein interactions are put to test in comparison to normal inhibitors.<sup>14</sup> To stimulate the development of new models, data sets of binding affinities

are required. Such a data set has recently been compiled for protein–protein complexes,<sup>15,16</sup> but no such data set is available for PPI inhibitors. Although docking and binding affinity prediction have been performed with success for specific systems,<sup>17–19</sup> a generic binding affinity prediction model for PPIs would be a welcome addition.

In this work, we report the optimization and performance of the HADDOCK score<sup>20,21</sup> on the prediction of the binding affinity of PPI inhibitors. This was performed on a binding affinity benchmark consisting of  $K_d$  and  $K_i$  values for 27 complexes from the 2P2I database.<sup>11,12</sup> In addition, we also compiled an independent set of PPI inhibitors for further validation, consisting of 19 protein–inhibitor complexes with available IC<sub>50</sub> data. Finally, we predicted the affinity of five different inhibitors that target the interaction between bromodomains and acetylated histones. We additionally investigate experimental ambiguity in affinity measurement and propose an acceptable prediction error on this basis. The original HADDOCK score, which is a linear combination of van der Waals and electrostatics energy terms calculated using the OPLS force field,<sup>22</sup> together with an additional empirical desolvation term,<sup>23</sup> was originally optimized for discriminating near-native poses in protein–protein docking.<sup>21</sup> We present here the PPI-optimized score, HADDOCK<sub>2P2I</sub>, which is shown to predict, close to experimental error (~2-fold larger), the binding affinities of PPI inhibitors. Its components provide valuable new insights into the determinants of the inhibition of PPIs.

Received: September 12, 2013

Published: February 12, 2014

Table 1.  $K_i$  and  $K_d$  Binding Affinity Data Set of Protein–Protein Interaction Inhibitors<sup>a</sup>

interaction	biological role	PDB (complex)	$K_d$ (complex) (M)	
Bcl-x <sub>L</sub> /Bak	programmed cell death	1bxl	$3.4 \times 10^{-7}$	
modulator (common name)	PubChem compound identifier (CID)	binding partner	PDB (complex)	$K_i  K_d$ (modulator) (M)
1 N3B	4369509	Bcl-x <sub>L</sub>	1ysi	$1.2 \times 10^{-7}$
2 ABT-737	11228183	Bcl-x <sub>L</sub>	2yxj	$5.0 \times 10^{-10}$
3 4FC	2782689	Bcl-x <sub>L</sub>	1ysg	$3.0 \times 10^{-5}$
4 TN1	68258	Bcl-x <sub>L</sub>	1ysg	$4.3 \times 10^{-3}$
5 LIU	15991562	Bcl-2	2o22	$6.7 \times 10^{-8}$
6 W1191542	44182311	Bcl-x <sub>L</sub>	3inq	$1.1 \times 10^{-8}$
interaction	biological role	PDB (complex)	$K_d$ (complex) (M)	
MDM2/p53	transcription regulation	1ycr	$6.0 \times 10^{-7}$	
modulator (common name)	PubChem compound identifier (CID)	binding partner	PDB (complex)	$K_i  K_d$ (modulator) (M)
7 HDM2	656933	MDM2	1t4e	$8.0 \times 10^{-8}$
8 WK23	44825260	MDM2	3lbk	$9.2 \times 10^{-7}$
9 MI-63	72200152	MDM2	3lbl	$3.6 \times 10^{-8}$
interaction	biological role	PDB (complex)	$K_d$ (complex) (M)	
XIAP-BIR3/CASPASE-9	programmed cell death	1nw9	$2.0 \times 10^{-8}$	
modulator (common name)	PubChem compound identifier (CID)	binding partner	PDB (complex)	$K_i  K_d$ (modulator) (M)
10 998	4369343	XIAP-BIR3	1tfq	$1.2 \times 10^{-8}$
11 997	5388929	XIAP-BIR3	1tft	$5.0 \times 10^{-9}$
12 9JZ	72199974	XIAP-BIR3	3hl5	$3.4 \times 10^{-5}$
interaction	biological role	PDB (complex)	$K_d$ (complex) (M)	
XIAP-BIR3/SMAC	programmed cell death	1g73	$4.2 \times 10^{-7}$	
modulator (common name)	PubChem compound identifier (CID)	binding partner	PDB (complex)	$K_i  K_d$ (modulator) (M)
13 B16	72199334	XIAP-BIR3	2jk7	$6.7 \times 10^{-8}$
14 AoxSPW	24916924	XIAP-BIR3	2opy	$3.0 \times 10^{-5}$
15 Smac005	25011737	XIAP-BIR3	3clx	$1.2 \times 10^{-7}$
16 Smac005	25011737	XIAP-BIR3	3cm7	$1.2 \times 10^{-7}$
17 Smac010	25011738	XIAP-BIR3	3cm2	$4.2 \times 10^{-7}$
18 Smac037	25058143	XIAP-BIR3	3eyl	$2.2 \times 10^{-7}$
19 CZ3	72199333	XIAP-BIR3	3g76	$2.3 \times 10^{-7}$
interaction	biological role	PDB (complex)	$K_d$ (complex) (M)	
ZipA/FtsZ	cell cycle regulation/cellular structure	1f47	$2.0 \times 10^{-5}$	
modulator (common name)	PubChem compound identifier (CID)	binding partner	PDB (complex)	$K_i  K_d$ (modulator) (M)
20 WAI	656967	ZipA	1y2f	$1.2 \times 10^{-5}$
21 CL3	5287936	ZipA	1y2g	$8.3 \times 10^{-5}$
interaction	biological role	PDB (complex)	$K_d$ (complex) (M)	
HPV-E2/E1	viral infection	1tue	n/d	
modulator (common name)	PubChem compound identifier (CID)	binding partner	PDB (complex)	$K_i  K_d$ (modulator) (M)
22 BILH 434	5287508	HPV-E2	1r6n	$4.0 \times 10^{-8}$
interaction	biological role	PDB (complex)	$K_d$ (complex) (M)	
IL-2/IL-2R	immune system regulation	1z92	$1.0 \times 10^{-8}$	
modulator (common name)	PubChem compound identifier (CID)	binding partner	PDB (complex)	$K_i  K_d$ (modulator) (M)
23 FRG	5288250	IL-2	1m48	$2.2 \times 10^{-5}$
24 FRB	23586028	IL-2	1pw6	$7.0 \times 10^{-6}$
25 SP-1985	5287951	IL-2	1m49	$7.5 \times 10^{-6}$
26 FRH	5288251	IL-2	1py2	$1.0 \times 10^{-7}$
27 SP-4160	656989	IL-2	1qvn	$1.4 \times 10^{-6}$

<sup>a</sup>Original references for the affinity data are provided in the Supporting Information (Table S1).

## MATERIALS AND METHODS

**Benchmark Compilation.** Information about available structural data for protein–protein interaction inhibitors was retrieved from the 2P2I database<sup>11</sup> (see Table 1) and the corresponding coordinates downloaded from the Protein Data Bank (www.pdb.org).<sup>24</sup> Binding affinity data (dissociation constants,  $K_d$  values, and inhibition constants,  $K_i$  values) were manually procured from literature (see Table 1 and associated references in Supporting Information Table S1). In total, data for 7 different protein–protein complexes were identified, for which 27 structures and binding affinity data of complexes with various PPI inhibitors were available.

**Structure Refinement.** The crystal structures of the inhibitors of PPIs in complex with their respective proteins were refined in HADDOCK<sup>20,21,25</sup> and subsequently scored. This ensured that all potentially missing side-chains were properly built and the interface of the complex was optimized using the OPLS force field.<sup>22</sup> For this, the standard water refinement setup in HADDOCK was used, which starts by solvating the complexes in an 8 Å shell of water molecules (TIP3P) and consists of the following steps:

(1) Energy minimization (EM) of the water, 40 steps with the protein fixed (Powell minimizer), followed by  $2 \times 40$  EM

steps with harmonic position restraints on the protein heavy atoms ( $k_{\text{rest}} = 5 \text{ kcal mol}^{-1} \text{ \AA}^{-2}$ ).

(2) Gentle simulated annealing protocol using molecular dynamics in Cartesian space consisting of

(a) a heating period with 500 MD steps at 100, 200, and 300 K with position restraints ( $k_{\text{rest}} = 5 \text{ kcal mol}^{-1} \text{ \AA}^{-2}$ ) on the protein heavy atoms except for the side-chains at the interface,

(b) a sampling stage with 1250 MD steps with weak ( $k_{\text{rest}} = 1 \text{ kcal mol}^{-1} \text{ \AA}^{-2}$ ) position restraints on the protein heavy atoms except for the backbone and side chains at the interface, and

(c) a cooling stage with 500 MD steps at 300, 200, and 100 K with weak ( $k_{\text{rest}} = 1 \text{ kcal mol}^{-1} \text{ \AA}^{-2}$ ) position restraints on the protein backbone heavy atoms not at the interface. A time step of 2 fs was used for the integration of the equation of motions and the temperature was maintained constant by weak coupling to a reference temperature bath using the Berendsen thermostat.<sup>26</sup>

(3) Final 200 EM steps without any position restraints.

Nonbonded interactions were calculated with the OPLS force field<sup>22</sup> using a cutoff of 8.5 Å. The electrostatic energy ( $E_{\text{elec}}$ ) was calculated using a shift function while a switching function (between 6.5 and 8.5 Å) was used for the van der Waals energy ( $E_{\text{vdw}}$ ). This procedure generated 20 models for each complex, starting from different random velocities. As is default in the HADDOCK protocol, the average score of the top 4 models was considered.

Table 2. IC50 Binding Affinity Data Set of Protein–Protein Interaction Inhibitors<sup>a</sup>

interaction	biological role	PDB (complex)	$K_d$ (complex) (M)		
Bcl-x <sub>L</sub> /Bak	programmed cell death	1bkl	$3.4 \times 10^{-7}$		
modulator (common name)	PubChem compound identifier (CID)	binding partner	PDB (complex)	IC50 (modulator) (M)	
28	H10	24798804	Bcl-x <sub>L</sub>	3qkd	$3.0 \times 10^{-09}$
29	0Q5	56973540	Bcl-x <sub>L</sub>	4ehr	$1.3 \times 10^{-08}$
interaction	biological role	PDB (complex)	$K_d$ (complex) (M)		
LEDGF/75-integrase	programmed cell death	2b4j	$1.1 \times 10^{-8}$		
modulator (common name)	PubChem compound identifier (CID)	binding partner	PDB (complex)	IC50 (modulator) (M)	
30	723	921795	75-integrase	3lpt	$1.2 \times 10^{-5}$
31	976	45281242	75-integrase	3lpu	$1.4 \times 10^{-6}$
32	TQ2	44199170	75-integrase	4e1m	$2.2 \times 10^{-7}$
33	TQX	44198672	75-integrase	4e1n	$1.9 \times 10^{-8}$
interaction	biological role	PDB (complex)	$K_d$ (complex) (M)		
MDM2/p53	transcription regulation	1ycr	$6 \times 10^{-7}$		
modulator (common name)	PubChem compound identifier (CID)	binding partner	PDB (complex)	IC50 (modulator) (M)	
34	IMY	49867154	MDM2	1ttv	$1.6 \times 10^{-7}$
35	YIN	5594130	MDM2	3jzk	$1.2 \times 10^{-6}$
36	OR2	56591324	MDM2	4ere	$4.2 \times 10^{-9}$
37	OR3	56965957	MDM2	4erf	$1.1 \times 10^{-9}$
38	BLF	56951871	MDM2	4dij	$3.0 \times 10^{-8}$
interaction	biological role	PDB (complex)	$K_d$ (complex) (M)		
TNF/TNF receptor	inflammation	n/d	n/d		

modulator (common name)	PubChem compound identifier (CID)	binding partner	PDB (complex)	IC50 (modulator) (M)	
39	703	4470566	TNF receptor	1ft4	$2.7 \times 10^{-7}$
interaction	biological role	PDB (complex)	$K_d$ (complex) (M)		
bromodomain/histone	inflammation	n/d	n/d		
modulator (common name)	PubChem compound identifier (CID)	binding partner	PDB (complex)	IC50 (modulator) (M)	
40	P9M	53054259	BRD2	4a9m	$5.0 \times 10^{-7}$
41	A9N	72200779	BRD2	4a9n	$1.5 \times 10^{-6}$
42	JQ1	46907787	BRD2	3oni	$1.3 \times 10^{-7b}$
43	JQ1	46907787	BRDT	4flp	$1.9 \times 10^{-7b}$
44	JQ1	46907787	BRD4	3mxf	$4.9 \times 10^{-8b}$
45	EAM	46943432	BRD4	3p5o	$5.1 \times 10^{-8b}$
46	I-BET151	52912189	BRD4	3zyu	$1.0 \times 10^{-7b}$
interaction	biological role	PDB (complex)	$K_d$ (complex) (M)		
integrin $\alpha$ -L/ICAM1 (CD-54)	host–virus interaction	1nw9	$2.0 \times 10^{-8}$		
modulator (common name)	PubChem compound identifier (CID)	binding partner	PDB (complex)	IC50 (modulator) (M)	
47	LA1	5326914	integrin $\alpha$ -L	1xuo	$6.9 \times 10^{-8}$
48	2O7	16040268	integrin $\alpha$ -L	2o7n	$1.5 \times 10^{-8}$
49	BQM	11712628	integrin $\alpha$ -L	3bqm	$1.7 \times 10^{-9}$
50	E2M	24875322	integrin $\alpha$ -L	3e2m	$0.4 \times 10^{-10}$
51	BJZ	11699447	integrin $\alpha$ -L	3m6f	$2.5 \times 10^{-9}$

<sup>a</sup>Original references for the IC50 data were retrieved from the relevant PDB entries in the Protein Data Bank (www.pdb.org). <sup>b</sup> $K_d$  data, retrieved from the Protein Data Bank (www.pdb.org).

All calculations were performed with HADDOCK, version 2.1/CNS,<sup>27</sup> version 1.2, through the refinement interface of the HADDOCK web server<sup>25</sup> (<http://haddock.science.uu.nl/services/HADDOCK/haddockserver-refinement.html>).

The same protocol can be run manually on a local installation of HADDOCK by turning off randomization of starting orientations, rigid body minimization and random removal of restraints and setting all steps for the semiflexible refinement stage (it1) to 0. This was used for the refinement runs using the ACPYPE parametrization of the ligands (see Results).

**HADDOCK<sub>2P21</sub> Model Development and Evaluation.** Multiple linear regression analysis was used to create the optimized HADDOCK<sub>2P21</sub> score based on the following equation:

$$\log K_{\text{pred}} = \text{HADDOCK}_{2P21} = \beta_1 E_{\text{vdw}} + \beta_2 E_{\text{elec}} + \beta_3 E_{\text{desolv}} + \beta_4 \text{BSA} + c \quad (1)$$

where  $E_{\text{vdw}}$  and  $E_{\text{elec}}$  denote the intermolecular van der Waals and electrostatics energies,  $E_{\text{desolv}}$  an empirical desolvation energy,<sup>23</sup> and BSA the buried surface area.  $\log K_{\text{pred}}$  denotes the logarithm of the predicted binding affinity of the inhibitors.

The  $\beta_i$  and  $c$  coefficients were optimized using 4-fold cross-validation by minimizing the  $\chi^2$  function (eq 2) for the 27 complexes shown in Table 1.

$$\chi^2 = \sum_{i=1}^{N_{\text{complex}}} [\log K_{\text{pred}}(i) - \log K_{\text{exp}}(i)]^2 \quad (2)$$

where  $K_{\text{exp}}$  corresponds to the experimentally measured  $K_d$  and  $K_i$  constants. During optimization, the various HADDOCK score components were switched on and off to assess their usefulness in the final development of the model. Similar parametrization methods have already been employed successfully for various protein–ligand systems to date.<sup>28–30</sup> The final coefficients were taken as the average of the 4-fold cross-validation optimization runs.

#### Independent Sets for Assessing the Prediction Performance of the HADDOCK Score and HADDOCK<sub>2P21</sub>

For compiling the training set and performing the 4-fold cross-validation, we carefully selected only competitive inhibitors, avoiding any noncompetitive modulators of the interactions. Data from interaction inhibition are often reported not as  $K_i$  (or, equivalently,  $K_d$ ), but instead as IC50, the latter denoting the concentration of ligand that reduces interaction activity by 50%. IC50 measures inhibitor binding in competition with another binding partner; consequently, it depends on the concentration of the competitive molecule and its affinity for the target protein. IC50s are usually larger than  $K_i$  values, but when the concentration of the substrate is very low, they should become essentially equal to  $K_i$ .<sup>31</sup> Since data about protein concentration in the assays were rather scarce we chose to omit complexes with only IC50 values from the training/cross-validation set. These were, however, included as an independent set for prediction, because of their different physicochemical but related nature. A list of 19 inhibitors of protein–protein interactions with known molecular structures

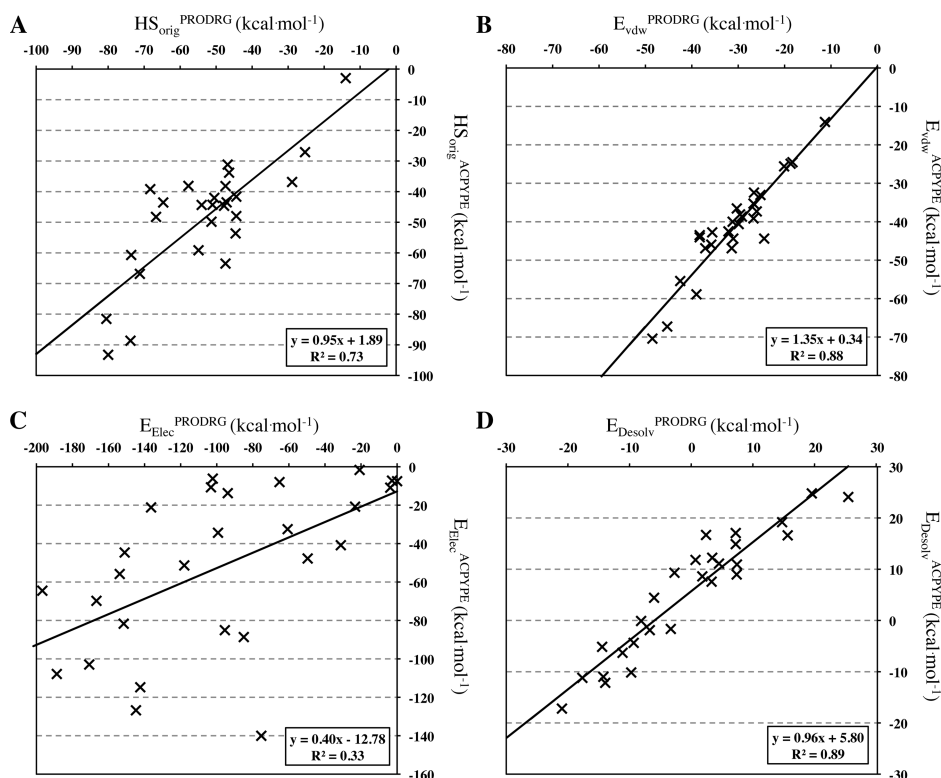


**Figure 1.** Correlation plots between energetic components calculated using ACPYPE and PRODRG-derived parameters. (A) Original HADDOCK score ( $E_{\text{vdw}} + 0.2E_{\text{elec}} + E_{\text{desol}}$ ), (B) van der Waals energy, (C) electrostatic energy, and (D) desolvation energy.

and IC50 values was manually procured from the literature using 2P2I database and iPPI-DB as starting points (Table 2).

Additionally, affinity predictions of inhibitors that target a protein–protein complex, not included in the training/cross-validation set were performed with HADDOCK<sub>2P2I</sub>. These inhibitors were designed to disrupt the interaction between bromodomains that specifically recognize  $\epsilon$ -N-acetylation of lysine residues, a post-translational modification common on histone tails. All interactions include measured  $K_d$  data and have available molecular structures in the Protein Data Bank (www.pdb.org).

**Estimation of Experimental Uncertainty and Qualitative Comparison to Prediction Error.** To assess the physicochemical relevance of the prediction error in the cross-validated set and the test sets used, we collected from the iPPI-DB<sup>10</sup> all interactions that fulfill the following criteria:

- (1) The same small molecule must inhibit the same interaction.
- (2) Two or more binding affinity measurements using different experimental methods should be available, but affinity constants must be of the same nature (e.g.,  $K_d$ ,  $K_i$ , or IC50).

We, therefore, compiled a data set of 72 interactions that match the above-mentioned criteria (Supporting Information Table S3). Estimation of experimental ambiguity of the derived data is performed using descriptive statistics and distribution analysis, and is empirically compared to the prediction accuracy.

**Assessment of the Structural Variability between Ligands and Proteins in the Data Set.** To verify that the protein–inhibitor complexes selected for both training and prediction were not structurally redundant, which meant the predictive ability of our biophysical model would be limited to a few classes of complexes, we carried out an analysis of the similarity between the ligands and the protein binders of each data sets. The protein similarity was assessed using sequence

similarity following a pairwise global alignment of the sequences (as taken from the RCSB PDB Web site) calculated with the Needleman–Wunsch algorithm available at the EBI Web site (www.ebi.ac.uk/Tools/psa/emboss\_needle/).<sup>32,33</sup> Features such as histidine tags from the purification protocol were not included in these calculations. Ligands were compared using a substructure key-based 2D Tanimoto similarity,<sup>34</sup> which was calculated via the PubChem score matrix web service (http://pubchem.ncbi.nlm.nih.gov/score\_matrix/score\_matrix.cgi).<sup>35</sup>

## RESULTS

We investigated the protein–protein complexes from the 2P2I database and collected from the literature affinity data for 27 inhibitors targeting 7 different protein–protein complexes.  $K_i$  and  $K_d$  data were combined into a single data set, excluding any IC50 measurements, which was manually curated and assembled from two different databases. These IC50 values and their respective complexes were used as a test set, to assess the performance of the developed functions in unknown cases, with fuzzier data.

**Compilation of a Structure-Based Data Set of PPI Inhibitors with Known  $K_i$  and  $K_d$  Data.** The resulting binding constants include  $K_d$  and  $K_i$  values describing the modulation/inhibition of the 7 protein–protein complexes (see Table 1). They span the range from very low (mM) to very high affinity (nM), covering thus a broad spectrum of potencies. For two of the complexes (Bcl-x<sub>L</sub>/Bak and SMAC-DIABLO/XIAP-BIR3), inhibitors with a large range of affinities have been cocrystallized. For example, the survival protein Bcl-x<sub>L</sub> in complex with the death-promoting region of the Bcl-2-related protein Bak<sup>36</sup> is a medium affinity complex ( $K_d = 340$  nM), whereas designed PPI inhibitors against it exhibit binding affinities from 4.3 mM to 0.5 nM. Another complex reported in this study is Smac/DIABLO bound to the third BIR



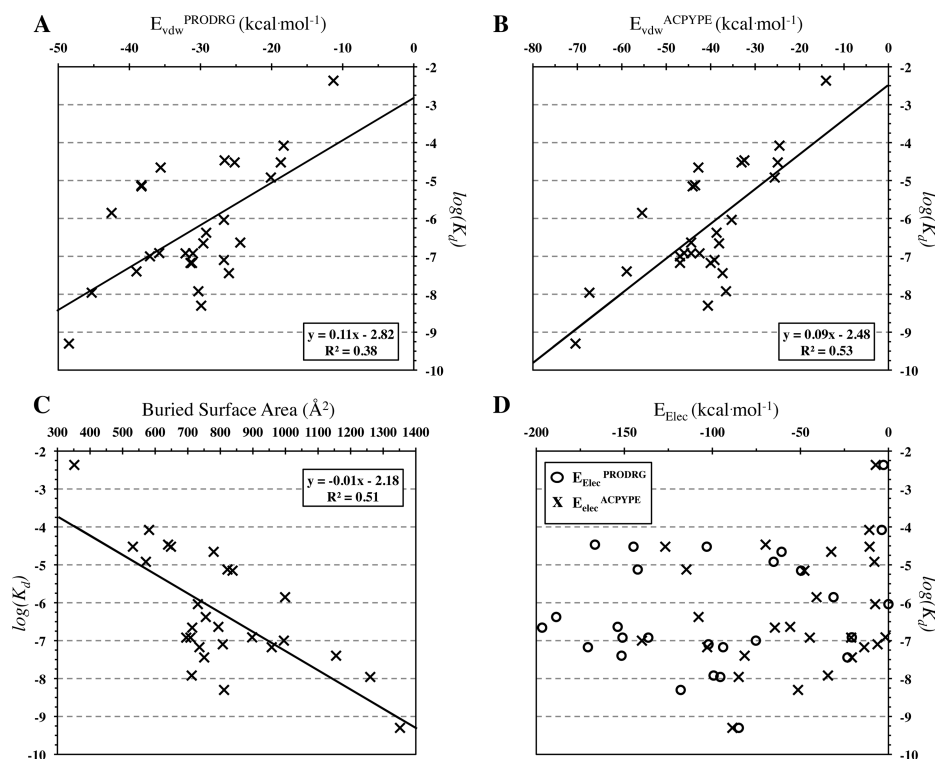


**Figure 2.** Correlation plots of experimentally determined binding affinities of PPI modulators with (A, B) the van der Waals energy calculated with the two ligand parametrization schemes, (C) the buried surface area (calculated using PRODRG parameters for the ligands), and (D) the electrostatic energy.

domain (BIR3) of XIAP, a complex critical for cellular apoptosis.<sup>37</sup> Its reported affinity is 420 nM, whereas inhibitors designed to disrupt this interaction cover a broad range of  $K_i$ , from 300 mM to 67 nM. For the other complexes reported in Table 1, fewer inhibitors with known  $K_i$  or  $K_d$  data have been reported; they exhibit various binding potencies.

**Evaluation of Force Field Topologies and Parameters for PPI Inhibitors.** The crystal structures of the PPI inhibitors in complex with their respective proteins were subjected to short refinement and scored using both the HADDOCK refinement web interface<sup>25</sup> and a local installation (see Methods). Force field topologies and parameters of all PPI inhibitors were generated using both PRODRG<sup>38</sup> and ACPYPE.<sup>39</sup> The main difference between the two tools is that, while PRODRG is based on a database search method to parametrize the molecules using OPLS-like parameters,<sup>22</sup> ACPYPE uses ANTECHAMBER<sup>40</sup> with a semiempirical quantum calculation method for the partial charges. A comparison of the original HADDOCK scores ( $HS_{\text{orig}} = E_{\text{vdw}} + 0.2E_{\text{elec}} + E_{\text{desolv}}$ ) of the complexes using these two parameter sets reveals differences (Figure 1A) ( $r^2 = 0.73$ ,  $N = 27$ ,  $p$ -value  $< 0.0001$ ), showing that ligand parameters play a substantial role in defining the interaction energy of each complex. While the desolvation ( $E_{\text{desolv}}$ ) and van der Waals energies ( $E_{\text{vdw}}$ ) are essentially identical ( $r^2 = 0.89$ ,  $N = 27$ ,  $p$ -value  $< 0.0001$  and  $r^2 = 0.88$ ,  $N = 27$ ,  $p$ -value  $< 0.0001$ , respectively) (Figure 1B and D), the electrostatic component ( $E_{\text{elec}}$ ) changes dramatically ( $r^2 = 0.33$ ,  $N = 27$ ,  $p$ -value = 0.0017) (Figure 1C) because of differences in partial charges. The buried surface area (BSA), which depends on the van der Waals radii, is however almost identical ( $r^2 = 0.98$ ,  $N = 27$ ,  $p$ -value  $< 0.0001$ , data not shown).

**Performance of HADDOCK Score in PPI Inhibitor Binding Affinity Prediction. Training and Cross-Validation of HADDOCK<sub>2P2I</sub>.** The individual components of  $HS_{\text{orig}}$  show

different contributions to the binding affinity with the van der Waals energy being the most significant contributor ( $r^2 = 0.53$ ,  $N = 27$ ,  $p$ -value  $< 0.0001$  for  $E_{\text{vdw}}^{\text{ACPYPE}}$  and  $r^2 = 0.38$ ,  $N = 27$ ,  $p$ -value = 0.0006 for  $E_{\text{vdw}}^{\text{PRODRG}}$ ) (Figure 2 A and B). The BSA also shows a strong positive correlation with binding affinity independently of the parametrization tool used ( $r^2 = 0.51$ ,  $N = 27$ ,  $p$ -value  $< 0.0001$ ) (Figure 2C). The electrostatic energy, in contrast, does not correlate to binding affinity ( $r^2 = 0.07$ ,  $N = 27$ ,  $p$ -value = 0.1823 for  $E_{\text{elec}}^{\text{ACPYPE}}$  and  $r^2 = 0.04$ ,  $N = 27$ ,  $p$ -value = 0.3172 for  $E_{\text{elec}}^{\text{PRODRG}}$ ) (Figure 2D).

In terms of binding affinity prediction using  $HS_{\text{orig}}$ , both parametrization schemes exhibit comparable results ( $r^2 = 0.40$ ,  $N = 27$ ,  $p$ -value = 0.0004) (Figure 3A and B).

The components of the original HADDOCK score, together with the BSA, which is used in HADDOCK in the scoring of the initial models at the rigid body stage, were optimized (see Methods) leading to the optimized HADDOCK score, termed HADDOCK<sub>2P2I</sub>. It is described by the following equation:

$$\begin{aligned} \text{HADDOCK}_{2P2I} &= \log K_{\text{pred}} \\ &= -0.006_{\pm 0.003} E_{\text{Elec}} - 0.018_{\pm 0.020} E_{\text{desolv}} \\ &\quad + 0.005_{\pm 0.001} \text{BSA} + 2.0_{\pm 0.9} \end{aligned} \quad (3)$$

Note that the parameters are averages from the 4-fold cross-validation. As can be seen from the standard deviations given as subscripts, there can be quite some variation in some parameters, in particular the weight of the desolvation term. The values of these coefficients may very well vary depending on the data set used for cross-validation; only a much larger data set (unfortunately not available) would allow a better convergence. Still, the model selected (eq 3) outperforms all other models tested (see Supporting Information Table S2), reaching an  $r^2 = 0.57$ ,  $N = 27$ ,  $p$ -value  $< 0.0001$  ( $r^2 = 0.53$ ,

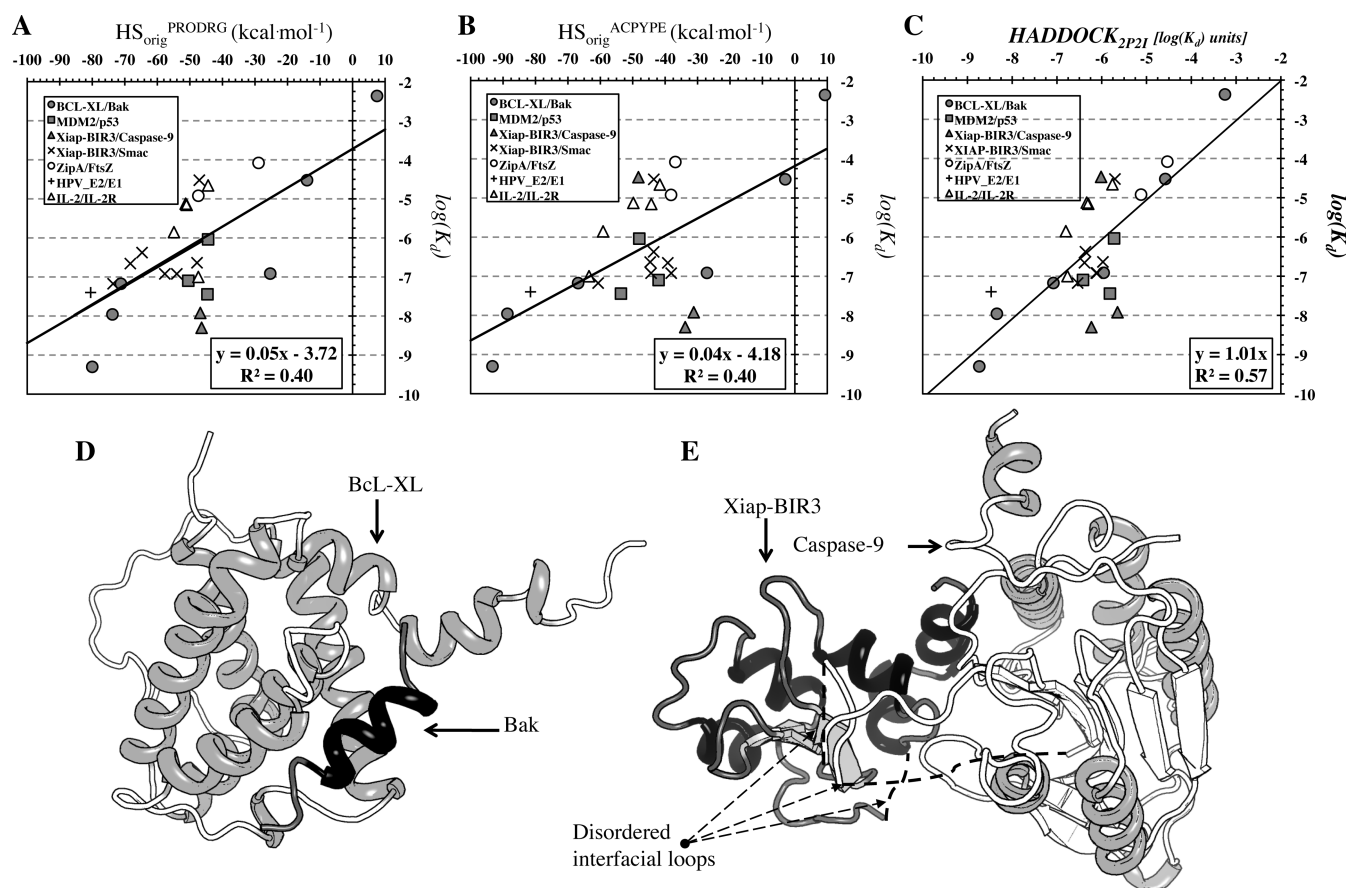


**Figure 3.** Correlation plots of experimentally determined binding affinities with the original HADDOCK score ( $E_{vdw} + 0.2E_{elec} + E_{desol}$ ) calculated with (A and B) the two parametrization schemes and (C) the optimized HADDOCK<sub>2P21</sub> score. (D and E) Cartoon representation of (D) the near-rigid Bcl-xL/Bak and (E) the flexible Xiap-BIR3/caspase-9 protein–protein complex.

$N = 27$ ,  $p$ -value  $< 0.0001$  after cross-validation) for complexes parametrized with PRODRG (Figure 3C) with a mean absolute error (MAE) of  $0.8 \pm 0.6$  kcal mol<sup>-1</sup>. It includes two of the original components of the HADDOCK score with an additional BSA term which substitutes the original van der Waals energy term. For complexes parametrized with ACPYPE, the model still retains its predictive capacity ( $r^2 = 0.45$ ,  $N = 27$ ,  $p$ -value = 0.0001 after cross-validation), albeit to a lesser extent (see Supporting Information Table S2). Note that the HADDOCK<sub>2P21</sub> scores from both parametrization schemes are very similar ( $r^2 = 0.88$ ,  $N = 27$ ,  $p$ -value  $< 0.0001$ ). The most notable difference compared to the original HADDOCK score, next to the difference in coefficients, is that the van der Waals energy term has been replaced by the Buried Surface Area term.

A protein–protein complex of central medical relevance is the one formed between the survival protein Bcl-x<sub>L</sub> and the death-promoting region of the Bcl-2-related protein Bak (Figure 3D). Proteins in the Bcl family are critical regulators of apoptosis and contain members that inhibit programmed cell death, such as Bcl-x<sub>L</sub> and Bcl-2. These proteins are overexpressed in many cancers and contribute to tumor initiation, progression, and resistance to therapeutics. Successful inhibition of this protein–protein interaction will have major consequences in cancer therapeutics.<sup>41</sup> Both the original ( $r^2 = 0.86$ ,  $N = 6$ ,  $p$ -value  $< 0.001$ ) and optimized ( $r^2 = 0.94$ ,  $N = 6$ ,  $p$ -value  $< 0.001$ ) HADDOCK scores are able to relate the scores of all six designed inhibitors for this particular complex

to their potency, with the optimized HADDOCK<sub>2P21</sub> performing slightly better (Figure 3 solid circles, compare A–C).

Although the model can, in general, efficiently predict affinity data for different inhibitors of protein–protein complexes, the prediction performance is directly influenced by conformational changes taking place upon binding: indeed, while for the rigid interface of the Bcl-XL/Bak complex discussed above (Figure 3D) predicted affinities are lying close to the regression line (solid circles in Figure 3C), in contrast, for the more flexible interface region of the Xiap-BIR3, that is also flexible in the interaction with Caspase 9 (Figure 3E), predicted affinities show a poor, or even lack of, correlation to experimental values (solid triangles in Figure 3C).

Last but not least, when we calculate the simple correlation between molecular weight of the inhibitor and its corresponding affinity, significant correlations emerge ( $r^2 = 0.43$ ,  $N = 27$ ,  $p$ -value = 0.0002), albeit weaker compared to the derived HADDOCK<sub>2P21</sub> score ( $r^2 = 0.51$ ,  $N = 27$ ,  $p$ -value  $< 0.0001$ ), indicating that 3D information is needed to more efficiently predict ligand affinities.

**Compilation of a Structure-Based Data Set for PPI Inhibitors with IC<sub>50</sub> Values. Prediction of IC<sub>50</sub> Data with the HADDOCK Score and HADDOCK<sub>2P21</sub>.** To assess the performance of both the original HADDOCK score and HADDOCK<sub>2P21</sub>, we compiled a data set of related affinity data that include a total of 19 protein–inhibitor complexes for 6 different protein–protein interactions (Table 2). Four complexes are new and have not been incorporated in the training/cross-validation set, including inhibitors of the interaction

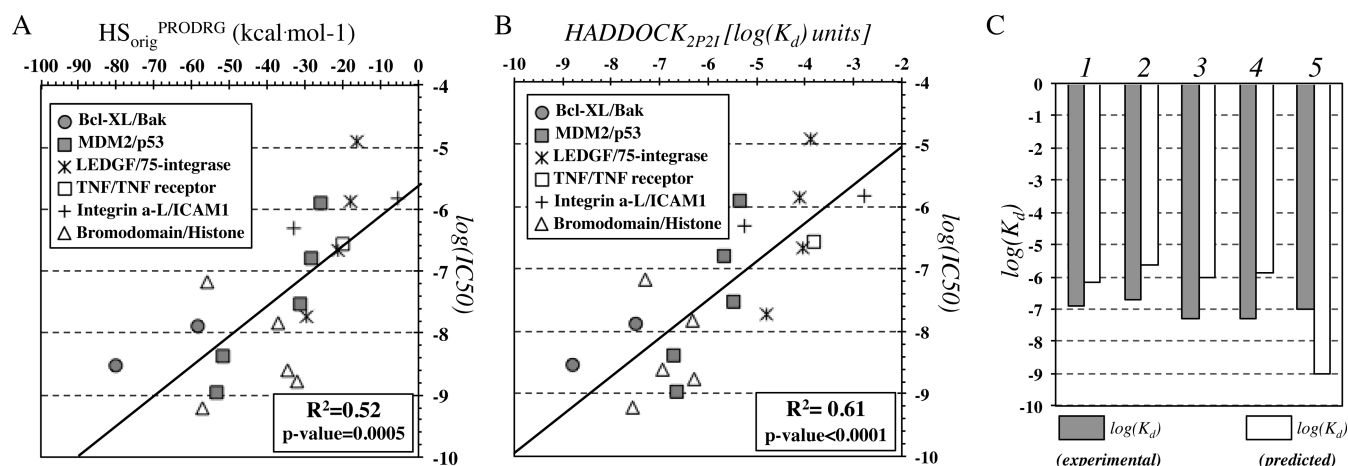


**Figure 4.** Correlation plots of experimentally determined binding affinities with (A) the original HADDOCK score ( $E_{\text{vdw}} + 0.2E_{\text{elec}} + E_{\text{desol}}$ ) and (B) the optimized HADDOCK<sub>2P21</sub> score. (C) Prediction of affinities for inhibitors of bromodomains that recognize acetylated histone tails for complexes 1–5 corresponding to PDB IDs 3ONI, 4FLP, 3MXF, 3P5O, and 3ZYU, respectively.

between human transcriptional coactivator p75 (LEDGF) and viral integrase. The derived inhibitors have corresponding IC<sub>50</sub>s ranging from 12  $\mu\text{M}$  to 19 nM. Tighter binding is exhibited by inhibitors of another host–virus interaction, that between a viral integrin and CD54, also known as Intercellular Adhesion Molecule 1 (ICAM 1), where IC<sub>50</sub>s span from 69 nM to 400 pM. Overall, the derived test set comprises different complexes with different binding constants, making this data set significantly distinct compared to the test/cross-validation set.

The best performance in predicting IC<sub>50</sub> data is obtained for HADDOCK<sub>2P21</sub> ( $r^2 = 0.61$ ,  $N = 19$ ,  $p$ -value < 0.0001) but predictions with the original HADDOCK score are also reliable ( $r^2 = 0.52$ ,  $N = 19$ ,  $p$ -value = 0.0005) (Figure 4A and B). Note, however, that these results should be treated with caution because the method was developed to reproduce  $K_d$  measurements in a quantitative manner and not IC<sub>50</sub> values. Unfortunately, we could not compile an independent test set of  $K_d$  or  $K_i$  data due to the absence of combined structural and affinity data for protein–protein interaction inhibitors. There is however a clear trend for HADDOCK<sub>2P21</sub> to relate to IC<sub>50</sub> values for different complexes. The molecular weight of these ligands also correlates with affinity ( $r^2 = 0.37$ ,  $N = 19$ ,  $p$ -value = 0.006), but the correlations with HADDOCK<sub>2P21</sub> are much better ( $r^2 = 0.61$ ,  $N = 19$ ,  $p$ -value < 0.0001), and those by the original HADDOCK score are also higher ( $r^2 = 0.52$ ,  $N = 19$ ,  $p$ -value = 0.0005). This confirms the need of structural information to gain additional insights into ligand affinity.

HADDOCK<sub>2P21</sub> was also used to predict  $K_d$  values for 5 known complexes of the same family and initially found in iPPI-DB. These data concern different bromodomains (BRD4, BRD2, BRDT), for which small-molecule inhibitors have been developed to disrupt their interaction with the *ε*-N-acetylated histone tails. Overall, the prediction of  $K_d$  for this set is reasonable, and the absolute mean error of the prediction is  $\sim 1.6$  kcal mol<sup>-1</sup> (Figure 4C). Note that the highest prediction error ( $\sim 1.9$  kcal mol<sup>-1</sup>) corresponds to the complex between BRD4 and I-BET151 (GSK1210151A) inhibitor. The complex buries an unusually large surface area (1351 Å<sup>2</sup>) that directly leads to higher predicted affinity. Note that large buried surface area in macromolecular complexation could be the outcome of extended conformational changes upon binding and, therefore, hamper accurate affinity estimation.<sup>16</sup>

#### Data Obtained from Different Experimental Methods Profoundly Limits the Prediction Accuracy.

The iPPI-DB<sup>10</sup> has the largest collection of affinity data for modulators/inhibitors of protein–protein interactions to date. It also includes affinity data for compounds targeting the same protein–protein interaction that were measured using different experimental methods. Multiple  $K_d$  data are rather scarce. Inhibition of the bromodomain 3 activity (BRD3) by compound entry 1603 in iPPI-DB was measured both by isothermal titration calorimetry (ITC) and surface plasmon resonance (SPR). A 4-fold difference between affinities was observed ( $K_d^{\text{ITC}} = 50$  nM,  $K_d^{\text{SPR}} = 200$  nM). For the same compound targeting the bromodomain 4 (BRD4) activity, a 6-fold difference in affinities was observed ( $K_d^{\text{ITC}} = 55$  nM,  $K_d^{\text{SPR}} = 324$  nM). Even measurements with the same biophysical methods can vary – as an example, compound entry 713 in iPPI-DB inhibits the XIAP-Smac interaction in the  $\mu\text{M}$  range, but measured data with fluorescence polarization (FP) reach a 1.3-fold difference in  $K_d$  ( $K_d^{\text{FP1}} = 0.275$   $\mu\text{M}$ ,  $K_d^{\text{FP2}} = 0.209$   $\mu\text{M}$ ).

IC<sub>50</sub> values obtained from various cellular assays are more abundant in the database. We have compiled a list that contains multiple IC<sub>50</sub> measurements for 72 interactions (Supporting Information Table S3). In particular, FP and fluorescence resonance energy transfer (TR-FRET) were used to measure inhibition of different bromodomains for a variety of ligands (Figure 5A). Correlation between methods is strong for individual bromodomains (BRD1  $r^2 = 0.76$ ,  $N = 9$ ,  $p$ -value = 0.002, BRD2  $r^2 = 0.80$ ,  $N = 9$ ,  $p$ -value = 0.001; BRD3  $r^2 = 0.88$ ,  $N = 8$ ,  $p$ -value = 0.001), but when considered together, the relation is less profound, explaining 72% of the data ( $r^2 = 0.72$ ,  $N = 26$ ,  $p$ -value < 0.0001). What is also clear is that IC<sub>50</sub>s obtained with TR-FRET are always of better affinity, reaching a 5-fold decrease in IC<sub>50</sub>, corresponding to 0.7 in  $-\log$  scale. Therefore, a correction of the relationship with an additional  $\beta$  parameter is needed ( $y = 0.7x + 1.9$ ,  $\beta = 1.9$ ) (Figure 5A); When modeling affinity, however, the biophysical data are not corrected by this additional parameter because we assume a 1:1 relation between affinities measured from different experimental methods. In that case, the derived relationships lead to much lower correlations, albeit still significant ( $r^2 = 0.54$ ,  $N = 26$ ,  $p$ -value < 0.0001) (Figure 5A). Similar conclusions have been made by experimentalists themselves, showing that 36 sulfonamides aiming to inhibit BRD4 activity exhibit similar



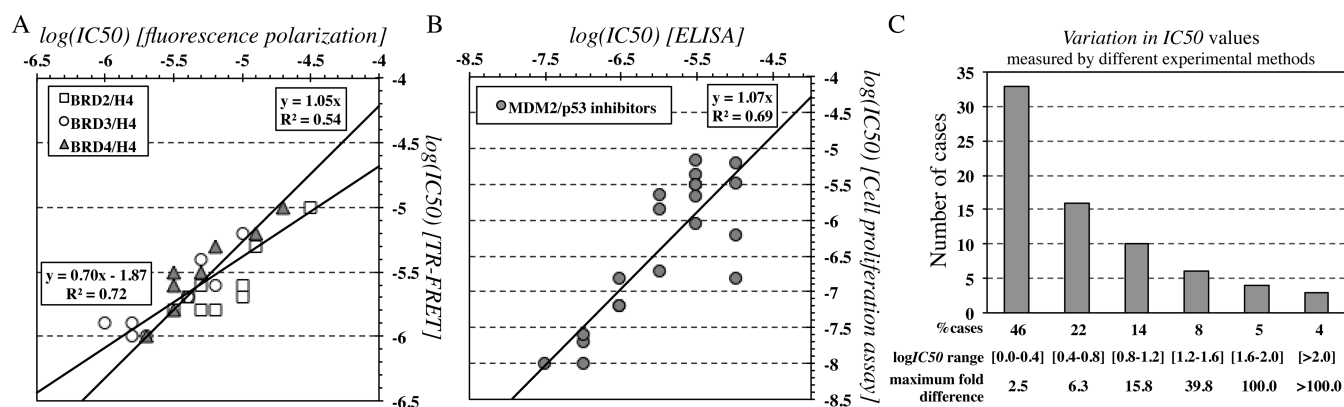


**Figure 5.** Assessment of experimental uncertainty in the determination of  $\text{IC}_{50}$  for PPI inhibitors using different assays. (A) Inhibitors of various bromodomains, measured by both fluorescence polarization and fluorescence resonance energy transfer (TR-FRET). Two regression lines are shown ( $y = ax + \beta$  and  $y = ax$ ), highlighting that absence of the  $\beta$  coefficient substantially lowers  $r^2$ . (B) Inhibitors of the MDM2/p53 interaction, measured by both ELISA and cell proliferation assays. (C) Distribution of fold differences in  $\text{IC}_{50}$  for 72 inhibitors targeting various protein–protein interactions that have been measured by two (or more) different experimental methods.

$\text{IC}_{50}$  values, but not identical between cell-based and biochemical assays ( $r^2 = 0.57$ ,  $N = 36$ ,  $p$ -value  $< 0.0001$ ).<sup>42</sup>

Another example is the inhibition of the MDM2/p53 interaction using different ligands and measured by both ELISA and cell proliferation assays (CPA) (Figure 5B); we observe that  $\text{IC}_{50}$  values do indeed correlate without adding a correction coefficient  $\beta$  to their linear relation ( $r^2 = 0.68$ ,  $N = 21$ ,  $p$ -value  $< 0.0001$ ), but measurements may differ by more than 2 orders of magnitude (e.g., for entry 1143 of iPPI-DB,  $\text{IC}_{50}^{\text{ELISA}} = 0.1 \mu\text{M}$ , and  $\text{IC}_{50}^{\text{CPA}} = 158 \mu\text{M}$ ).

The distribution of the overall ambiguity in affinity measurements is shown in Figure 5C for all 72 entries with multiple experimental measurements collected from iPPI-DB (Supporting Information Table S3). Nearly half of the interactions measured have an ambiguity of  $< 0.4$  in  $-\log \text{IC}_{50}$  units, which corresponds to less than 2-fold changes in  $\text{IC}_{50}$ . The other half of the data exhibit deviations in  $\text{IC}_{50}$ s by more than 2-fold, reaching a maximum of 1650-fold change, the latter representing changes in  $-\log \text{IC}_{50}$  by 3.2 units. Overall, the average experimental uncertainty for these data is rather low,  $0.7 \pm 0.7$   $-\log \text{IC}_{50}$  units, with a median of  $0.5$   $-\log \text{IC}_{50}$  units and a maximum of  $3.2$   $-\log \text{IC}_{50}$  units.

Considering such deviations in  $-\log \text{IC}_{50}$  units for a single system using two independent measurements, the prediction error of HADDOCK<sub>2P21</sub> on the validation set ( $0.8 \pm 0.6 \text{ kcal mol}^{-1}$ ), on the “fuzzy”  $\text{IC}_{50}$  test set ( $1.6 \pm 0.9 \text{ kcal mol}^{-1}$ ) and the  $K_d$  set concerning inhibition of different bromodomains ( $1.3 \pm 0.5 \text{ kcal mol}^{-1}$ ), is in the same range of accuracy as experimental uncertainty.

## DISCUSSION

HADDOCK<sub>2P21</sub> is a biophysical model optimized to predict the binding affinities of inhibitors of PPIs. By optimizing the weights of the original HADDOCK score and including a BSA term, the resulting model is able to predict binding affinities of PPI inhibitors close to experimental error ( $\sim 2$ -fold larger). To test this, we have compiled from iPPI-DB and analyzed a set of binding affinities obtained with various experiments for the same system. We have estimated an experimental uncertainty for  $\text{IC}_{50}$  values of  $0.7 \pm 0.7$  in  $-\log \text{IC}_{50}$  units (based on 72 data points), with a maximum of  $3.2$   $-\log \text{IC}_{50}$  units, the latter seemingly rare. Experimental conditions can also influence binding affinity determination, especially changes in pH.

However, modeling the effect of pH was outside the scope of this study; this might well, if properly accounted for, lower the prediction error. Although the effect of pH on the binding affinity of PPI inhibitors is unclear at this time, it is known that for protein–protein complexes, changing the pH by three units, changes the  $K_d$  by a factor of 10–50, and  $\Delta G$  by  $1.4$ – $2.3 \text{ kcal mol}^{-1}$ .<sup>16</sup>

Despite those limitations, our algorithm reasonably reproduces a variety of experimental affinities of different nature ( $\text{IC}_{50}$ ,  $K_i$ ,  $K_d$ ) for distinct protein–protein interaction inhibitors. Since new PPI inhibitors are regularly published and crystallized with associated biophysical measurements for their interaction, this leaves room for further optimization of our HADDOCK<sub>2P21</sub> binding affinity predictor. One could possibly argue that, because of the limited size of the data set, the prediction capacity of HADDOCK<sub>2P21</sub> is not generalizable. Previous studies on scoring functions for “classical” protein–ligand complexes have shown that such limited amount of training data leads to a bias, which could only be surpassed when more than 100 cases are available in a data set.<sup>43</sup> The diversity of the data as well as number of predictor variables used may also influence the results. To exclude a potential lack of diversity, we performed a similarity analysis of the proteins and ligands included in both training/cross-validation and test sets; this highlights the diversity of the studied systems and reflects their nonredundancy (Figure 6). Even for systems that have highly homologous protein structures, single mutations in the sequence, being directly at the interface or not, are often observed that could have implications in the binding energies of the ligands.

In this work, two different ligand parametrization tools were compared: a semi-quantum mechanical approach (ACPYPE), and the faster, database-driven PRODRG. Both parametrization schemes yield similar performance in terms of binding affinity prediction using the optimized HADDOCK score, with PRODRG slightly outperforming ACPYPE. The main difference between the two sets of parameters resides in the electrostatics partial charges. While this might not affect much affinity prediction based on refined crystal structures, it might well have a much more profound impact on docking results, something that should be evaluated in the future.

The prediction performance for PPI inhibitors seems somewhat better than that of the most recent protein–



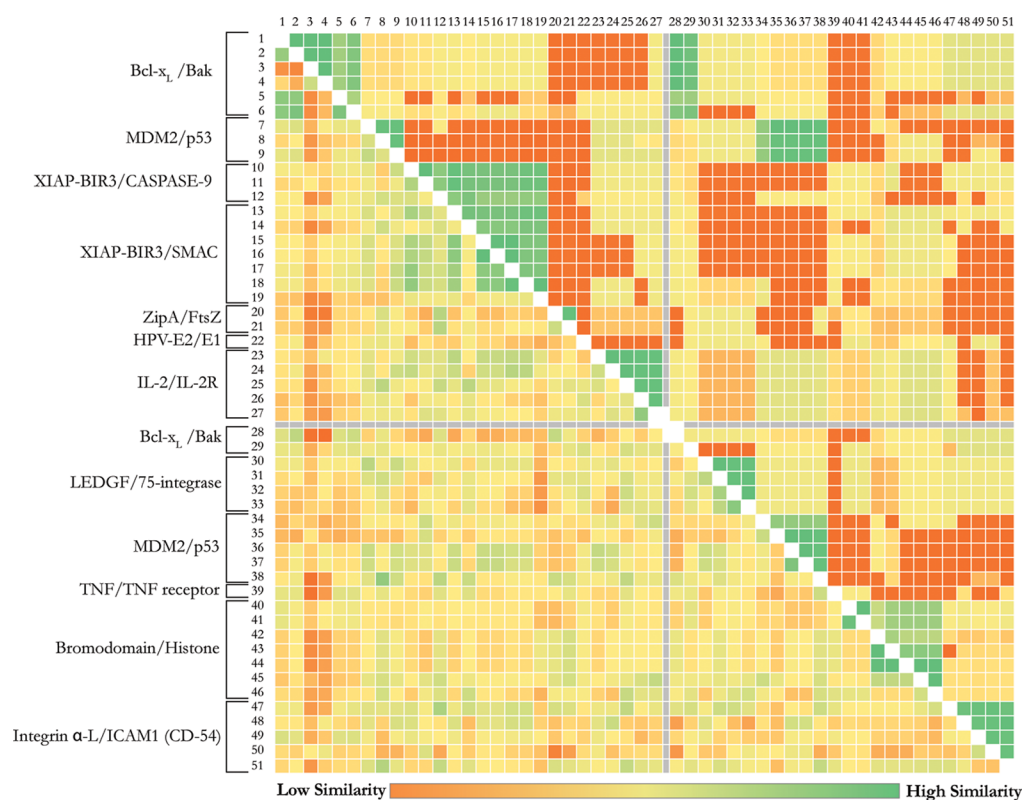


**Figure 6.** All-versus-all similarity analysis for the proteins<sup>33</sup> and their bound inhibitors<sup>34</sup> of the used data set, highlighting the diversity in the systems under study (shown at the left of the matrix). The upper-right and the lower-left halves of the matrix represent the all-versus-all similarity for the proteins and their bound inhibitors, respectively. Rows and columns 1–27 and 28–51 correspond to the training/cross-validation set and the independent test set, respectively (following numbering introduced in Tables 1 and 2).

ligand/drug design program. The latter, when tested against new blind data sets, showed a predictive capacity ranging from  $r^2 = 0.30$  to  $0.40$ .<sup>44,45</sup> For a fair comparison, HADDOCK<sub>2P21</sub> and other small ligand binding affinity models should be tested against similar data sets. One test set used in this study contains IC50 data; these cannot be related to actual  $K_d$  or  $K_i$  measurements from biophysical methods, since substrate Michaelis constant ( $K_m$ ) and related concentration must be reported ( $S$ ), assuming the inhibitor is competitive. If  $S \ll K_m$ , then  $K_i \approx IC50$ , but again, verification from classical biophysical methods is advisable.

PPI inhibitors differ in nature from small molecule inhibitors that target enzymes and it remains to be seen how well the optimized function presented here will predict small molecule binding affinities (which was outside the scope of this work).

Next to yielding an optimized function for binding affinity prediction, this study also provides new insights into the determinants of the binding affinity of PPI inhibitors. In particular, affinity prediction deteriorates as a function of conformational freedom of the system under study, directly pointing to missing entropic contributions (Figure 3C–E). These results are similar in nature with the ones we derived for protein–protein complexes and with the impact of conformational change on binding affinity prediction.<sup>15,16</sup> Nevertheless, the buried surface area (BSA) and van der Waals interactions show moderate-to-high correlations with binding affinity data for all complexes tested. The two are of course directly correlated. The desolvation and electrostatic energies show more complicated profiles than just plain correlation. This does not mean that they do not contribute per se: both the original and optimized models for the HADDOCK score clearly show a

direct contribution of these two components, albeit to a smaller extent than the BSA: The BSA contributes on average,  $3.6 \pm 1.3$  kcal mol<sup>-1</sup> to the overall HADDOCK<sub>2P21</sub> score, whereas the contributions of electrostatics and desolvation only reach  $0.5 \pm 0.4$  and  $0.1 \pm 0.2$  kcal mol<sup>-1</sup>, respectively, when calculated over the entire validation data set.

The BSA and van der Waals interactions are features that were already known to be critical factors for the affinity of protein–ligand<sup>46</sup> and protein–protein complexes.<sup>47,48</sup> The correlations calculated in this study for the BSA of inhibitors of protein–protein interactions are, however, substantially higher than the ones calculated for protein–protein complexes,<sup>16</sup> but smaller than for standard protein–ligand complexes.<sup>46</sup> This indicates that, in designing highly affine inhibitors of PPIs, one should aim at optimizing the complementarity of the inhibitors with the protein interface and always consider conformational changes as these are a limiting factor for accurate prediction.<sup>49</sup> In conclusion, the newly designed score, HADDOCK<sub>2P21v</sub>, should facilitate and guide the design of PPI inhibitors, especially for the less flexible interfaces.

## ■ ASSOCIATED CONTENT

### 📄 Supporting Information

Details of the data set of binding affinity data for protein–protein interaction inhibitors (Table S1), details of the optimization of the HADDOCK score (Table S2), and associated affinities for systems that were measured by two of more methods (Table S3). This material is available free of charge via the Internet at <http://pubs.acs.org>.

## AUTHOR INFORMATION

## Corresponding Author

\*E-mail: a.m.j.bonvin@uu.nl. Telephone: +31302533859. Fax: +31302537623.

## Present Address

<sup>†</sup>Panagiotis L. Kastritis: EMBL Heidelberg, Meyerhofstraße 1, 69117 Heidelberg, Germany, Tel. +49 6221 387–8107.

## Author Contributions

The manuscript was written through contributions of all authors. All authors have given approval to the final version of the manuscript.

## Notes

The authors declare no competing financial interest.

## ACKNOWLEDGMENTS

This work was supported by the Dutch Foundation for Scientific Research (NWO) through a VICI grant (No. 700.56.442) and a Focus and Massa grant from Utrecht University. The authors thank the many biochemists who measured the binding constants used in this article.

## REFERENCES

- (1) Costanzo, M.; Baryshnikova, A.; Bellay, J.; Kim, Y.; Spear, E. D.; Sevier, C. S.; Ding, H.; Koh, J. L.; Toufighi, K.; Mostafavi, S.; Prinz, J.; St Onge, R. P.; VanderSluis, B.; Makhnevych, T.; Vizeacoumar, F. J.; Alizadeh, S.; Bahr, S.; Brost, R. L.; Chen, Y.; Cokol, M.; Deshpande, R.; Li, Z.; Lin, Z. Y.; Liang, W.; Marback, M.; Paw, J.; San Luis, B. J.; Shuteriqi, E.; Tong, A. H.; van Dyk, N.; Wallace, I. M.; Whitney, J. A.; Weirauch, M. T.; Zhong, G.; Zhu, H.; Houry, W. A.; Brudno, M.; Ragibzadeh, S.; Papp, B.; Pal, C.; Roth, F. P.; Giaever, G.; Nislow, C.; Troyanskaya, O. G.; Bussey, H.; Bader, G. D.; Gingras, A. C.; Morris, Q. D.; Kim, P. M.; Kaiser, C. A.; Myers, C. L.; Andrews, B. J.; Boone, C. The genetic landscape of a cell. *Science* **2010**, *327*, 425–431.
- (2) Vidal, M.; Cusick, M. E.; Barabasi, A. L. Interactome networks and human disease. *Cell* **2011**, *144*, 986–998.
- (3) Mullard, A. Protein–protein interaction inhibitors get into the groove. *Nat. Rev. Drug Discovery* **2012**, *11*, 173–175.
- (4) Koes, D. R.; Camacho, C. J. PocketQuery: Protein–protein interaction inhibitor starting points from protein–protein interaction structure. *Nucleic Acids Res.* **2012**, *40*, W387–W392.
- (5) Koes, D.; Khoury, K.; Huang, Y.; Wang, W.; Bista, M.; Popowicz, G. M.; Wolf, S.; Holak, T. A.; Domling, A.; Camacho, C. J. Enabling large-scale design, synthesis and validation of small molecule protein–protein antagonists. *PLoS One* **2012**, *7*, No. e32839.
- (6) Koes, D. R.; Camacho, C. J. Small-molecule inhibitor starting points learned from protein–protein interaction inhibitor structure. *Bioinformatics* **2012**, *28*, 784–791.
- (7) Reynes, C.; Host, H.; Camproux, A. C.; Laconde, G.; Leroux, F.; Mazars, A.; Deprez, B.; Fahraeus, R.; Villoutreix, B. O.; Sperandio, O. Designing focused chemical libraries enriched in protein–protein interaction inhibitors using machine-learning methods. *PLoS Comput. Biol.* **2010**, *6*, No. e1000695.
- (8) Villoutreix, B. O.; Labbe, C. M.; Lagorce, D.; Laconde, G.; Sperandio, O. A leap into the chemical space of protein–protein interaction inhibitors. *Curr. Pharm. Des.* **2012**, *18*, 4648–4667.
- (9) Morelli, X.; Bourgeas, R.; Roche, P. Chemical and structural lessons from recent successes in protein–protein interaction inhibition (2P2I). *Curr. Opin. Chem. Biol.* **2011**, *15*, 475–481.
- (10) Labbe, C. M.; Laconde, G.; Kuenemann, M. A.; Villoutreix, B. O.; Sperandio, O. iPPI-DB: A manually curated and interactive database of small non-peptide inhibitors of protein–protein interactions. *Drug Discovery Today* **2013**, *18*, 958–968.
- (11) Bourgeas, R.; Basse, M. J.; Morelli, X.; Roche, P. Atomic analysis of protein–protein interfaces with known inhibitors: the 2P2I database. *PLoS One* **2010**, *5*, No. e9598.
- (12) Basse, M. J.; Betzi, S.; Bourgeas, R.; Bouzidi, S.; Chetrit, B.; Hamon, V.; Morelli, X.; Roche, P. 2P2IDb: A structural database dedicated to orthosteric modulation of protein–protein interactions. *Nucleic Acids Res.* **2013**, *41*, D824–D827.
- (13) Tuffery, P.; Derreumaux, P. Flexibility and binding affinity in protein–ligand, protein–protein and multi-component protein interactions: limitations of current computational approaches. *J. R. Soc., Interface* **2012**, *9*, 20–33.
- (14) Kruger, D. M.; Jessen, G.; Gohlke, H. How good are state-of-the-art docking tools in predicting ligand binding modes in protein–protein interfaces? *J. Chem. Inf. Model.* **2012**, *52*, 2807–2811.
- (15) Kastritis, P. L.; Bonvin, A. M. Are scoring functions in protein–protein docking ready to predict interactomes? Clues from a novel binding affinity benchmark. *J. Proteome Res.* **2010**, *9*, 2216–2225.
- (16) Kastritis, P. L.; Moal, I. H.; Hwang, H.; Weng, Z.; Bates, P. A.; Bonvin, A. M.; Janin, J. A structure-based benchmark for protein–protein binding affinity. *Protein Sci.* **2011**, *20*, 482–491.
- (17) Zhong, S.; Macias, A. T.; MacKerell, A. D., Jr. Computational identification of inhibitors of protein–protein interactions. *Curr. Top. Med. Chem.* **2007**, *7*, 63–82.
- (18) Metz, A.; Pflieger, C.; Kopitz, H.; Pfeiffer-Marek, S.; Baringhaus, K. H.; Gohlke, H. Hot spots and transient pockets: predicting the determinants of small-molecule binding to a protein–protein interface. *J. Chem. Inf. Model.* **2012**, *52*, 120–133.
- (19) Dezi, C.; Carotti, A.; Magnani, M.; Baroni, M.; Padova, A.; Cruciani, G.; Macchiarulo, A.; Pellicciari, R. Molecular interaction fields and 3D-QSAR studies of p53-MDM2 inhibitors suggest additional features of ligand–target interaction. *J. Chem. Inf. Model.* **2010**, *50*, 1451–1465.
- (20) de Vries, S. J.; van Dijk, A. D.; Krzeminski, M.; van Dijk, M.; Thureau, A.; Hsu, V.; Wassenaar, T.; Bonvin, A. M. HADDOCK versus HADDOCK: New features and performance of HADDOCK2.0 on the CAPRI targets. *Proteins* **2007**, *69*, 726–733.
- (21) Dominguez, C.; Boelens, R.; Bonvin, A. M. HADDOCK: A protein–protein docking approach based on biochemical or biophysical information. *J. Am. Chem. Soc.* **2003**, *125*, 1731–1737.
- (22) Jorgensen, W. L.; Tirado-Rives, J. T. The OPLS force field for proteins. Energy minimizations for crystals of cyclic peptides and crambin. *J. Am. Chem. Soc.* **1988**, *110*, 1657–1666.
- (23) Fernandez-Recio, J.; Totrov, M.; Abagyan, R. Identification of protein–protein interaction sites from docking energy landscapes. *J. Mol. Biol.* **2004**, *335*, 843–865.
- (24) Dutta, S.; Burkhardt, K.; Swaminathan, G. J.; Kosada, T.; Henrick, K.; Nakamura, H.; Berman, H. M. Data deposition and annotation at the worldwide protein data bank. *Methods Mol. Biol.* **2008**, *426*, 81–101.
- (25) de Vries, S. J.; van Dijk, M.; Bonvin, A. M. The HADDOCK web server for data-driven biomolecular docking. *Nat. Protoc.* **2010**, *5*, 883–897.
- (26) Berendsen, H. J. C.; Postma, J. P. M.; van Gunsteren, W. F.; DiNola, A.; Haak, J. R. Molecular dynamics with coupling to an external bath. *J. Chem. Phys.* **1984**, *8*, 3684–3690.
- (27) Brunger, A. T.; Adams, P. D.; Clore, G. M.; DeLano, W. L.; Gros, P.; Grosse-Kunstleve, R. W.; Jiang, J. S.; Kuszewski, J.; Nilges, M.; Pannu, N. S.; Read, R. J.; Rice, L. M.; Simonson, T.; Warren, G. L. Crystallography NMR system: A new software suite for macromolecular structure determination. *Acta Crystallogr. D. Biol. Crystallogr.* **1998**, *54*, 905–921.
- (28) Gilson, M. K.; Zhou, H. X. Calculation of protein–ligand binding affinities. *Annu. Rev. Biophys. Biomol. Struct.* **2007**, *36*, 21–42.
- (29) Singh, N.; Warshel, A. Absolute binding free energy calculations: On the accuracy of computational scoring of protein–ligand interactions. *Proteins* **2010**, *78*, 1705–1723.
- (30) Zhou, R.; Friesner, R. A.; Ghosh, A.; Rizzo, R. C.; Jorgensen, W. L.; Levy, R. M. New linear interaction method for binding affinity calculations using a continuum solvent model. *J. Phys. Chem. B* **2001**, *105*, 10388–10397.
- (31) Cheng, Y.; Prusoff, W. H. Relationship between the inhibition constant (K<sub>1</sub>) and the concentration of inhibitor which causes 50%

inhibition (I50) of an enzymatic reaction. *Biochem. Pharmacol.* **1973**, *22*, 3099–3108.

(32) Rice, P.; Longden, I.; Bleasby, A. EMBOSS: The European Molecular Biology Open Software Suite. *Trends Genet.* **2000**, *16*, 276–277.

(33) Needleman, S. B.; Wunsch, C. D. A general method applicable to the search for similarities in the amino acid sequence of two proteins. *J. Mol. Biol.* **1970**, *48*, 443–453.

(34) Rogers, D. J.; Tanimoto, T. T. A computer program for classifying plants. *Science* **1960**, *132*, 1115–1118.

(35) Bolton, E.; Wang, Y.; Thiessen, P. A.; Bryant, S. H. PubChem: Integrated platform of small molecules and biological activities. *Annu. Rep. Comput. Chem.* **2008**, *4*, 217–241.

(36) Sattler, M.; Liang, H.; Nettessheim, D.; Meadows, R. P.; Harlan, J. E.; Eberstadt, M.; Yoon, H. S.; Shuker, S. B.; Chang, B. S.; Minn, A. J.; Thompson, C. B.; Fesik, S. W. Structure of Bcl-xL-Bak peptide complex: Recognition between regulators of apoptosis. *Science* **1997**, *275*, 983–986.

(37) Shiozaki, E. N.; Chai, J.; Rigotti, D. J.; Riedl, S. J.; Li, P.; Srinivasula, S. M.; Alnemri, E. S.; Fairman, R.; Shi, Y. Mechanism of XIAP-mediated inhibition of caspase-9. *Mol. Cell* **2003**, *11*, 519–527.

(38) Schuttelkopf, A. W.; van Aalten, D. M. PRODRG: A tool for high-throughput crystallography of protein–ligand complexes. *Acta Crystallogr. D Biol. Crystallogr.* **2004**, *60*, 1355–1363.

(39) Sousa da Silva, A. W.; Vranken, W. F. ACPYPE—AnteChamber PYthon Parser interface. *BMC Res. Notes* **2012**, *5*, 367.

(40) Case, D. A.; Cheatham, T. E., 3rd; Darden, T.; Gohlke, H.; Luo, R.; Merz, K. M., Jr.; Onufriev, A.; Simmerling, C.; Wang, B.; Woods, R. J. The Amber biomolecular simulation programs. *J. Comput. Chem.* **2005**, *26*, 1668–1688.

(41) Lessene, G.; Czabotar, P. E.; Colman, P. M. BCL-2 family antagonists for cancer therapy. *Nat. Rev. Drug. Discovery* **2008**, *7*, 989–1000.

(42) Bamborough, P.; Diallo, H.; Goodacre, J. D.; Gordon, L.; Lewis, A.; Seal, J. T.; Wilson, D. M.; Woodrow, M. D.; Chung, C. W. Fragment-based discovery of bromodomain inhibitors part 2: optimization of phenylisoxazole sulfonamides. *J. Med. Chem.* **2012**, *55*, 587–596.

(43) Wang, R.; Liu, L.; Lai, L.; Tang, Y. SCORE: A new empirical method for estimating the binding affinity of a protein–ligand complex. *J. Mol. Model.* **1998**, *4*, 379–394.

(44) Cheng, T.; Li, X.; Li, Y.; Liu, Z.; Wang, R. Comparative assessment of scoring functions on a diverse test set. *J. Chem. Inf. Model.* **2009**, *49*, 1079–1093.

(45) Warren, G. L.; Andrews, C. W.; Capelli, A. M.; Clarke, B.; LaLonde, J.; Lambert, M. H.; Lindvall, M.; Nevins, N.; Semus, S. F.; Senger, S.; Tedesco, G.; Wall, I. D.; Woolven, J. M.; Peishoff, C. E.; Head, M. S. A critical assessment of docking programs and scoring functions. *J. Med. Chem.* **2006**, *49*, 5912–5931.

(46) Olsson, T. S.; Williams, M. A.; Pitt, W. R.; Ladbury, J. E. The thermodynamics of protein–ligand interaction and solvation: Insights for ligand design. *J. Mol. Biol.* **2008**, *384*, 1002–1017.

(47) Murphy, K. P.; Freire, E. Thermodynamics of structural stability and cooperative folding behavior in proteins. *Adv. Protein Chem.* **1992**, *43*, 313–361.

(48) Kastiris, P. L.; Bonvin, A. M. On the binding affinity of macromolecular interactions: daring to ask why proteins interact. *J. R. Soc., Interface* **2013**, *10*, No. 20120835.

(49) Kastiris, P. L.; Bonvin, A. M. Molecular origins of binding affinity: seeking the Archimedean point. *Curr Opin Struct Biol* **2013**, *23*, 868–877.